Articles

Contribution from the Lehrstuhl für Anorganische Chemie I der Ruhr-Universität, D-4630 Bochum, Federal Republic of Germany

Adiabatic Intramolecular Electron Transfer in Pyrazine-2,6-dicarboxylato-Bridged Complexes of Cobalt(III)–Ruthenium(II) and of Cobalt(III)–Iron(II): Comparison of Inner-Sphere vs. Outer-Sphere Activated Complexes

ADEMIR NEVES, WILLY HERRMANN, and KARL WIEGHARDT*

Received March 20, 1984

Intramolecular electron-transfer rate constants in the binuclear complex $[(NH_3)_5Ru^{II}–L_1–Co^{III}(dien)]^{3+}$ and in the series $[(NC)_5Fe^{II}–L_1–Co^{III}L_2]^{2-}$ (L_1 equals μ-pyrazine-2,6-dicarboxylate as bridging ligand and L_2 equals diethylenetriamine (dien), 3 NH_3, or *N*-(3-aminopropyl)-1,3-propanediamine (dpt)) have been measured. Specific rates at 25 °C are 0.059, 6.85 × 10^{-3}, 0.041, and 0.18 s^{-1}, respectively. It is concluded that electron transfer in these systems approaches the adiabatic regime. The kinetics of outer-sphere oxidation of $[Ru^{II}(NH_3)_5(pyraz\text{-}2,6\text{-}H_2)]^{2+}$ (pyraz-2,6-H_2 is pyrazine-2,6-carboxylic acid N-coordinated to Ru(II)) by various cobalt(III) complexes containing two tridentate ligands $[Co^{III}A_1B_1]^+$ (A_1 = pyrazine-2,6-dicarboxylate or pyridine-2,6-dicarboxylate; B_1 = 3 NH_3, dien, dpt) have been measured. All reactants exhibit reversible or quasi-reversible cyclic voltammograms. Electron-transfer self-exchange rates for $[Ru(NH_3)_5(pyraz\text{-}2,6\text{-}H_2)]^{2+/3+}$ and $[Co(dien)(pyraz\text{-}2,6)]^{+/0}$ have been elucidated to be 3.2 × 10^6 and 3.4 × 10^{-3} M^{-1} s^{-1} at 25 °C, respectively. The intramolecular electron-transfer rate constant for the outer-sphere reaction of $[(NC)_5Fe^{II}(pyraz\text{-}2,6\text{-}H)]^{4-}$ with $[Co(dien)(pyraz\text{-}2,6)]^+$ has been determined experimentally at 25 °C to be 0.039 s^{-1}, which is 5.7 times faster than is observed for the analogous inner-sphere complex $[(NC)_5Fe^{II}(pyraz\text{-}2,6)Co(dien)]^{2-}$. The same reactivity difference (6.8) has been deduced for the intramolecular electron transfer in the outer-sphere activated complexes $[(NH_3)_5Ru^{II}(pyraz\text{-}2,6\text{-}H_2)]^{2+}$, $[Co(dien)(pyraz\text{-}2,6)]^+$ and the inner-sphere complex $[(NH_3)_5Ru^{II}(\mu\text{-}pyraz\text{-}2,6)Co(dien)]^{3+}$. It is shown that these reactivity differences between outer-sphere and inner-sphere activated complexes are accounted for by the difference of driving force, with the assumption that $k_{et} \approx K^{1/2}$. This suggests that the outer-sphere reactions are also in the adiabatic regime, which may be achieved by electronic coupling within a stacked ion-pair or encounter complex.

Introduction

Taube and co-workers[1–5] have reported in a series of papers on the rates of intramolecular electron transfer in redox-active complexes of the inner-sphere type

$$[X(NH_3)_{4/5}Ru^{II}–L–Co^{III}(NH_3)_5]^{n+}$$

where X = H_2O or SO_4^{2-} and L are N-heterocyclic aromatic bridging ligands such as 4,4′-bipyridines, imidazolate, nicotinate or isonicotinate, pyrazine, and pyrazinecarboxylate. Relatively few cases have been reported to date on such systems using the more simple $Ru^{II}(NH_3)_5$ moiety as reductant.[6–8]

Haim[9–14] and Malin[15,16] and co-workers have subsequently developed a system that also allowed the measurement of intramolecular electron-transfer rate constants using the $Fe^{II}(CN)_5$ moiety as reductant in precursor complexes of the type

$$[(NC)_5Fe^{II}–L–Co^{III}(NH_3)_{4/5}]^{n-}$$

where L are the same N-heterocyclic aromatic bridging ligands as were used in the Co(III)–Ru(II) system.

Intramolecular electron transfer through the intact two first coordination spheres of outer-sphere type encounter complexes or ion pairs has been observed for complexes of cobalt(III) or ruthenium(III) being the oxidants and hexacyanoferrate(II)[19] or pentacyano(N-heterocycle)ferrate(II)[20] the reductants.

When the bridging ligand holds the redox-active metal centers in inner-sphere type precursor complexes at a close and rigid distance, as is the case for pyrazine or pyrazinecarboxylate bridging ligands, it has been suggested that the limiting adiabatic regime has been reached.[4,13] Experimental difficulties due to photo-induced rather than thermal electron transfer have prohibited the elucidation of the intramolecular electron-transfer rate constant[4] of $[(H_2O)Ru(NH_3)_4(\mu\text{-}pyrazinecarboxylate)Co(NH_3)_5]^{4+}$.

We here report a detailed study of intramolecular electron-transfer processes using pyrazine-2,6-dicarboxylate as ligand (N-coordinated to Ru(II) or Fe(II) and O,N,O-coordinated to Co(III)) or as bridging ligand between Fe(II)–Co(III) and Ru(II)–Co(III), respectively. We studied the intramolecular electron-transfer processes in comparable systems containing structurally very similar inner-sphere and outer-sphere complexes, e.g. within the ion pairs I and II and the precursors III and IV.

(1) Isied, S. S.; Taube, H. *J. Am. Chem. Soc.* **1973**, *95*, 8198.
(2) Fischer, H.; Tom, G. M.; Taube, H. *J. Am. Chem. Soc.* **1976**, *98*, 5512.
(3) Rieder, K.; Taube, H. *J. Am. Chem. Soc.* **1977**, *99*, 7891.
(4) Zawacky, S. K. S.; Taube, H. *J. Am. Chem. Soc.* **1981**, *103*, 3379.
(5) Isied, S. S.; Kuehn, C. G. *J. Am. Chem. Soc.* **1978**, *100*, 6754.
(6) Isied, S. S. In "Mechanistic Aspects of Inorganic Reactions"; Rorabacher, D. B., Endicott, J. F., Eds.; American Chemical Society: Washington, DC, 1982; ACS Symp. Ser. No. 198; p 221.
(7) Isied, S. S.; Worosila, G.; Atherton, S. J. *J. Am. Chem. Soc.* **1982**, *104*, 7659.
(8) Winkler, J. R.; Nocera, D. G.; Yocom, K. M.; Bordignon, E.; Gray, H. B. *J. Am. Chem. Soc.* **1982**, *104*, 5798.
(9) Gaswick, D.; Haim, A. *J. Am. Chem. Soc.* **1974**, *96*, 7845.
(10) Iwo, J.; Haim, A. *J. Am. Chem. Soc.* **1976**, *98*, 1172.
(11) Szecsy, A.; Haim, A. *J. Am. Chem. Soc.*: (a) **1981**, *103*, 1679; (b) **1982**, *104*, 3063.
(12) Iwo, J.; Gaus, P. L.; Haim, A. *J. Am. Chem. Soc.* **1979**, *101*, 6189.
(13) Haim, A. *Pure Appl. Chem.* **1983**, *55*, 89.
(14) Haim, A. *Prog. Inorg. Chem.* **1983**, *30*, 273.
(15) Malin, J. M.; Ryan, D. A.; O'Halloran, T. V. *J. Am. Chem. Soc.* **1978**, *100*, 2097.
(16) Piering, D. A.; Malin, J. M. *J. Am. Chem. Soc.* **1976**, *98*, 6045.
(17) Toma, H. E. *J. Inorg. Nucl. Chem.* **1975**, *37*, 785.
(18) Gaswick, D.; Haim, A. *J. Am. Chem. Soc.* **1971**, *93*, 7347.
(19) Miralles, A. J.; Armstrong, R. E.; Haim, A. *J. Am. Chem. Soc.* **1977**, *99*, 1416.
(20) Oliveira, L. A. A.; Giesbrecht, E.; Toma, H. E. *J. Chem. Soc., Dalton Trans.* **1979**, 236.

0020-1669/84/1323-3435$01.50/0

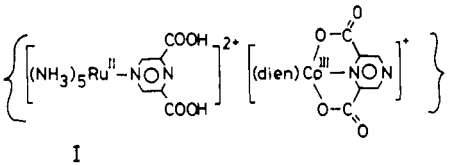

I

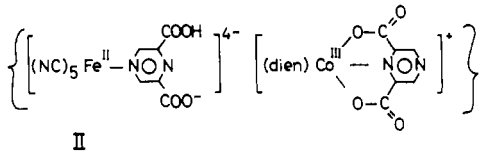

II

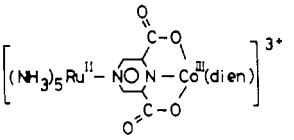

III

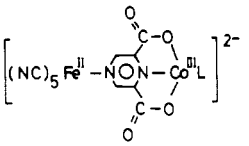

L= dien IVa
3 NH_3 IVb
dpt IVc

In addition, complexes IVa–c allow a study of the effect of varying nonbridging ligands coordinated to the oxidizing Co(III) center on the rate of intramolecular electron transfer. Since the formal redox potentials of the mononuclear cobalt(III) complexes $[Co^{III}(pyraz\text{-}2,6)L]^+$ (L = dien, dpt) can be measured by cyclic voltammetry, this should enable an indirect verification of the frequently used assumption that the intramolecular rate constant varies with driving force, $k_{et} \approx K^{1/2}$, a relation found for outer-sphere electron-transfer reactions (Marcus cross-reaction).

Experimental Section

Abbreviations of Ligands: dien = *N*-(2-aminoethyl)-1,2-ethanediamine or diethylenetriamine; dpt = *N*-(3-aminopropyl)-1,3-propanediamine ($C_6H_{17}N_3$); pyraz-2,6 = pyrazine-2,6-dicarboxylate ($C_6H_2N_2O_4$); dipic = pyridine-2,6-dicarboxylate ($C_7H_3NO_4$), pyraz-2,6-H and pyraz-2,6-H_2 = mono- and diprotonated forms of pyrazine-2,6-dicarboxylate; nic = nicotinate; isonic = isonicotinate; imz = imidazolate; pyraz = pyrazine.

Preparation of Pyrazine-2,6-dicarboxylic Acid. This ligand was prepared according to a published procedure involving decarboxylation of pyrazine-2,3,5-tricarboxylic acid.[21]

Preparation of Cobalt(III) Complexes. Monomeric complexes of the type $[Co(pyraz\text{-}2,6)L](ClO_4)$, where L = 3 NH_3, dien, dpt, were prepared by the following method: Pyrazine-2,6-dicarboxylic acid was dissolved in 10 mL of 0.5 M $HClO_4$ at 70 °C. $[Co(NH_3)_3(H_2O)Cl_2]Cl$,[22] $[Co(dien)Cl_3]$, or $[Co(dpt)Cl_3]$[23] (0.6 g) was added, respectively.

The solutions were kept at 60 °C for 10 min. To the filtered solutions was added 0.8 g of $NaClO_4$. Red crystals precipitated at 5 °C, which were filtered off, washed with ethanol and ether, and air-dried. The complexes were recrystallized twice from 0.1 M $HClO_4$. The yields were better than 80% in all cases. In the case of the $[Co^{III}(pyraz\text{-}2,6)(NH_3)_3]^+$ complex the rather insoluble chloride salt precipitated, which was converted to the more soluble perchlorate salt. The chloride salt (13 g) was dissolved in H_2O (400 mL at 60 °C), and $NaClO_4$ (400 g) was added. The perchlorate salt precipitated upon cooling to 5 °C.

[Co(dipic)(dien)]Cl was prepared from 0.6 g of $[Co(dien)Cl_3]$ dissolved in an aqueous hydrochloric acid solution (0.5 M; 20 mL) of pyridine-2,6-dicarboxylic acid (0.3 g) at 70 °C. The temperature was maintained at 60 °C for 10 min. NaCl (0.3 g) was added, and the solution was cooled to 5 °C. After 2 h red crystals were filtered off, which were recrystallized from 0.1 M HCl; yield 80%.

[Co(dipic)(dpt)]$(ClO_4)\cdot 3H_2O$. Pyridine-2,6-dicarboxylic acid (0.3 g) was dissolved in 0.5 M $HClO_4$ (10 mL) at 70 °C. $[Co(dpt)Cl_3]$ (0.6 g) was added in small amounts at 60 °C with stirring. After 10 min $NaClO_4$ (0.8 g) was added and the filtered solution was cooled to 10 °C. Red crystals precipitated, which were recrystallized from 0.1 M $HClO_4$; yield 80%.

Preparation of Ruthenium Complexes. $[Ru(NH_3)_5(pyraz\text{-}2,6\text{-}H_2)](ClO_4)_2\cdot 1.5H_2O$. $[Ru(NH_3)_5OH_2](PF_6)_2$[24] (0.2 g) was added to a solution (5 mL) of pyrazine-2,6-dicarboxylic acid (0.2 g) at pH 4 under an argon atmosphere at 20 °C. To the deep red solution were added 0.5 mL of 0.5 M $HClO_4$ and 0.5 g of $NaClO_4$. The solution was kept for 1 h at 5 °C. Red crystals were filtered off; yield 65%.

$[Ru(NH_3)_5(pyraz\text{-}2,6\text{-}H_2)](ClO_4)_3\cdot H_2O$ was obtained from the above red solution after addition of 3–5 drops of H_2O_2 (30%). The yellow solution was cooled to 5 °C. Pale yellow crystals were filtered off and washed with ethanol and ether; yield 70%. This material is light sensitive and decomposes slowly even when kept in the dark.

Preparation of $[(NH_3)_5Ru(\mu\text{-}pyraz\text{-}2,6)Co(dien)](ClO_4)_4$. $[Ru(NH_3)_5(pyraz\text{-}2,6\text{-}H_2)](ClO_4)_3\cdot H_2O$ (0.24 g) was dissolved in 5 mL of 0.5 M $HClO_4$ at 60 °C. $[Co(dien)Cl_3]$ (0.3 g) was added with stirring. The preparation was carried out with exclusion of light. After 10 min at 60 °C, $NaClO_4$ was added (0.5 g) and the solution was kept at 5 °C for 2 h. Red crystals were filtered off and were recrystallized from a minimum amount of 0.1 M $HClO_4$; yield 45%.

Preparation of $[Fe^{II}(CN)_5(pyraz\text{-}2,6)]^{5-}$. The complex was prepared in situ from solutions of $[Fe(CN)_5(OH_2)]^{3-}$ ($\sim 10^{-5}$ M) and pyrazine-2,6-dicarboxylic acid ($\sim 10^{-3}$ M) at pH 6. Solutions of $[Fe(CN)_5OH_2]^{3-}$ were obtained by aquation of $[Fe(CN)_5NH_3]^{3-}$ according to Haim's and Malin's procedure.[10,25] $[Fe(CN)_5(pyraz\text{-}2,6)]^{5-}$ exhibits an intense absorption maximum at 478 nm ($\epsilon = 4.8 \times 10^3$ L mol^{-1} cm^{-1}). Such solutions of the complex are stable to ligand dissociation for at least 24 h.[17]

Elemental analyses of all new complexes are available as supplementary material.

Kinetic Measurements. The kinetics of the outer-sphere reactions between $[Ru^{II}(NH_3)_5(pyraz\text{-}2,6\text{-}H_2)]^{2+}$ and $[Co^{III}L_1,L_2]^+$ (L_1 = pyridine-2,6-dicarboxylate or pyrazine-2,6-dicarboxylate; L_2 = 3 NH_3 or dien or dpt) were measured by conventional spectrophotometric methods (Unicam SP 1700 interfaced to a PET 2001 Commodore computer for data acquisition and analysis). All reactions were run under pseudo-first-order conditions with the oxidant in large excess over the reductant. Pseudo-first-order rate constants were calculated by using a least-squares program[26] where the absorptions at the beginning and after the completed reaction were treated as variables. The observed and calculated values differed only within the uncertainty

Scheme I

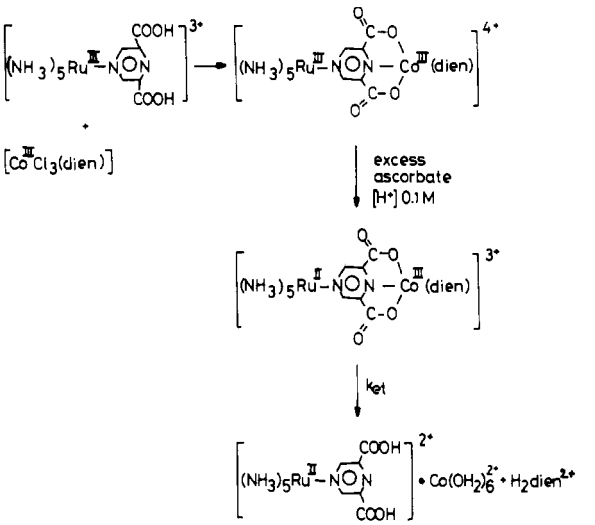

(21) Mager, H. I. X.; Berends, W. *Recl. Trav. Chim. Pays-Bas* **1958**, *77*, 827.
(22) Linhard, M.; Siebert, H. *Z. Anorg. Allg. Chem.* **1969**, *364*, 24.
(23) Searle, G. H.; Hambley, T. W. *Aust. J. Chem.* **1982**, *35*, 1297.
(24) Kuehn, C.; Taube, H. *J. Am. Chem. Soc.* **1975**, *98*, 689.
(25) Toma, H. E.; Malin, J. M. *Inorg. Chem.* **1974**, *13*, 1772.
(26) DeTar, D. F. *Comput. Chem.* **1979**, *2*, 99.

Table I. Electronic Spectra of the Complexes

complex	λ_{max}, nm (ϵ, L mol^{-1} cm^{-1})
$[Co(pyraz\text{-}2,6)(NH_3)_3]^+$	542 (231)[a]
$[Co(pyraz\text{-}2,6)(dien)]^+$	524 (232)[a]
$[Co(pyraz\text{-}2,6)(dpt)]^+$	550 (215)[a]
$[Co(dipic)(dien)]^+$	520 (200)[a]
$[Co(dipic)(dpt)]^+$	544 (235)[a]
$[Ru^{II}(NH_3)_5(pyraz\text{-}2,6\text{-}H_2)]^{2+}$	538 (1×10^4)[b]
$[Ru^{II}(NH_3)_5(pyraz\text{-}2,6)]^0$	506 (1×10^4)[c]
$[Ru^{III}(NH_3)_5(\mu\text{-}pyraz\text{-}2,6)Co(dien)]^{4+}$	524 (250)[a]
$[Ru^{II}(NH_3)_5(\mu\text{-}pyraz\text{-}2,6)Co(dien)]^{3+}$	576 (1.3×10^4)[a]
$[Fe^{II}(CN)_5(pyraz\text{-}2,6\text{-}H)]^{4-}$	512 (4.5×10^3)[d]
$[Fe^{II}(CN)_5(pyraz\text{-}2,6)]^{5-}$	478 (4.8×10^3)
$[Fe^{II}(CN)_5(\mu\text{-}pyraz\text{-}2,6)Co(dien)]^{2-}$	648 (7.3×10^3)

[a] Measured in water. [b] Measured in 0.2 M $HClO_4$. [c] Measured in acetate buffer (pH ~5). [d] Measured in citrate buffer (pH ~3).

of the last digit of the reading of the instrument. The reproducibility of replicate runs was better than 3% for all reactions. The kinetics of the outer-sphere reaction between $[Co(pyraz\text{-}2,6)(dien)]^+$ and $[Fe(CN)_5(pyraz\text{-}2,6\text{-}H)]^{4-}$ have been measured analogously. The reductant has been prepared in situ from $[Fe(CN)_5H_2O]^{3-}$ (10^{-5} M) and pyrazinedicarboxylic acid (10^{-3} M) at pH 6, and the oxidant was in large excess over the reductant.

The intramolecular $[(CN)_5Fe^{II}(\mu\text{-}pyraz\text{-}2,6)Co^{III}L]^{2-}$, rate constant of $[Ru^{II}(NH_3)_5(\mu\text{-}pyraz\text{-}2,6)Co^{III}dien]^{3+}$ has been measured following the procedure described by Zawacky and Taube.[4] Aqueous solutions of the precursor complex $[Ru^{III}(NH_3)_5(\mu\text{-}pyraz\text{-}2,6)Co^{III}dien]^{4+}$ ((1–3) $\times 10^{-5}$ M) were treated with excess reductant ascorbic acid (10^{-4}–10^{-3} M) in 0.1 M $HClO_4$. Thus, the process

$$Ru^{II}\text{–}L\text{–}Co^{III} + \text{reductant} \rightarrow Ru^{II}\text{–}L + Co^{2+} + \text{oxidized product} \quad (1)$$

has been followed spectrophotometrically at 600 nm for 6–8 half-lives.

The complexes $[(CN)_5Fe^{II}(\mu\text{-}pyraz\text{-}2,6)Co^{III}L]^{2-}$, where L = 3 NH_3, dien, dpt, were prepared in situ by combining freshly prepared solutions of $[Fe(CN)_5H_2O]^{3-}$ (10^{-5} M) and of $[Co(pyraz\text{-}2,6)L]^+$ ((0.6–2.0) $\times 10^{-3}$ M) to form the respective binuclear complexes at pH 4.5–6. The binuclear species were characterized by rapid formation of an intense blue color. The fading of this color was followed spectrophotometrically at 660 nm as a function of time. The latter process is ascribed to the thermal intramolecular electron transfer from Fe(II) to Co(III). In order to avoid complications arising from side reactions of the produced Fe(III) product with unreacted Fe(II)–Co(III) precursor complex, the reaction was run with excess ascorbate (10^{-3} M) and excess edta (5×10^{-4} M) to avoid precipitation of (Co^{II}/$Fe^{II}(CN)_5$-containing products, although this precaution proved to be unnecessary because the $[Fe^{II}(CN)_5(pyraz\text{-}2,6\text{-}H_2)]^{3-}$ complex is very stable in solution. Thus, the overall reaction (2) was followed.

$$[(CN)_5Fe^{II}(\mu\text{-}pyraz\text{-}2,6)Co^{III}L]^{2-} + \text{reductant} \xrightarrow{k_{ox}} [Fe^{II}(CN)_5(pyraz\text{-}2,6)]^{5-} + [Co^{II}L(OH_2)_3]^{2+} + \text{oxidized products} \quad (2)$$

Plots of ln $(A_t - A_\infty)$ vs. time were linear for at least 5 half-lives, and therefore first-order rate constants k_{obsd} were obtained from a nonlinear least-squares fitting with k and A_∞ being adjustable parameters.[26] The observed first-order rate constants were found to be independent of the concentration of the excess component $[Co^{III}L\text{-}(pyraz\text{-}2,6)]^+$ and independent of the concentration of added ascorbate (8×10^{-5}–1×10^{-3} M).

Electrochemistry. Cyclic voltammetric experiments were made with a Princeton Applied Research Model 173 potentiostat–galvanostat driven by a Model 175 universal programmer. Voltammograms were recorded on a Kipp & Zonen X-Y recorder, Model BD 90. The electrochemical cell used was a conventional three-electrode type with an aqueous Ag/AgCl (saturated KCl) electrode as a reference electrode and a platinum wire as the auxiliary electrode. As working electrode a hanging mercury drop electrode or a glassy-carbon electrode was used.

Argon-scrubbed aqueous solutions of complexes (10^{-3} M) containing a 0.1 M supporting electrolyte (acetate buffer, $HClO_4$, or $LiClO_4$) were measured at scan rates ranging from 10 to 500 mV s^{-1} at 25 °C. The measurements of pH dependence of redox potentials were performed in mixtures of $HClO_4/LiClO_4$ at 25 °C.

The half-wave potentials were calculated by using the midpoint of the anodic and cathodic peaks of reversible (or quasi-reversible) cyclic voltammograms. Redox potentials reported are all vs. the normal hydrogen electrode (NHE).

Results

Electronic Spectra. The visible absorption spectrum of $[Ru^{II}(NH_3)_5(pyraz\text{-}2,6\text{-}H_2)]^{2+}$ measured in 0.2 M $HClO_4$ at 25 °C shows an intense maximum at 538 nm ($\epsilon = 1 \times 10^4$ L mol^{-1} cm^{-1}) whereas at pH 5.0 (acetate buffer) the absorption maximum of the doubly deprotonated form, $[Ru^{II}\text{-}(NH_3)_5(pyraz\text{-}2,6)]^0$, is shifted to 506 nm. This indicates that protonation of the carboxylic groups strengthens the $Ru^{II} \rightarrow L$ back-bonding. Similar behavior is observed for $[Fe^{II}(CN)_5\text{-}(pyraz\text{-}2,6)]^{5-}$ and $[Fe^{II}(CN)_5(pyraz\text{-}2,6\text{-}H)]^{4-}$, which exhibit absorption maxima at 478 and 512 nm, respectively.

Coordination of a cobalt(III) center into the tridentate bite of the pyrazine-2,6-dicarboxylato ligand in $[Ru^{II}(NH_3)_5(py\text{-}raz\text{-}2,6\text{-}H_2)]^{2+}$ and in $[Fe^{II}(CN)_5(pyraz\text{-}2,6\text{-}H_2)]^{3-}$ to yield the binuclear complexes $[(NH_3)_5Ru^{II}(\mu\text{-}pyraz\text{-}2,6)Co^{III}(dien)]^{3+}$ and $[(NC)_5Fe^{II}(\mu\text{-}pyraz\text{-}2,6)Co^{III}(dien)]^{2-}$ causes a remarkably large bathochromic shift of the M^{II}–pyraz-2,6 charge-transfer band as compared to the monomeric Ru(II) and Fe(II) species, respectively. Similar spectral behavior has been observed in many related systems[4,10,11,17] and reflects the increased electron delocalization in the binuclear species.

Electrochemistry. The monomeric cobalt complexes containing two tridentate chelating ligands, $[Co^{III}L_1L_2]^+$ where L_1 = pyridine-2,6-dicarboxylate, pyrazine-2,6-dicarboxylate and L_2 = dien, dpt, exhibit reversible or quasi-reversible cyclic voltammograms. The redox potentials span a range from 0.085 to 0.335 V for the couples $[Co(dien)(pyr\text{-}2,6)]^{+/0}$ and $[Co\text{-}(dpt)(pyraz\text{-}2,6)]^{+/0}$, respectively. The results are summarized in Table II. The peak-potential differences, ΔE_p, are rather large, 65–85 mV, as compared to the theoretical value of 60 mV typical for a reversible one-electron transfer. This is an electrode-kinetic effect frequently observed in cyclic voltam-

Table II. Formal Reduction Potentials of Complexes

couple	medium[c]	ΔE_p,[b] mV	$E_{1/2}$,[a] V	$I_{p,a}/I_{p,c}$[e]
$[Co(dien)(pyraz\text{-}2,6)]^{+/0}$	B	80	0.24	0.78[f]
$[Co(dpt)(pyraz\text{-}2,6)]^{+/0}$	B	85	0.335	0.76[f]
$[Co(dien)(dipic)]^{+/0}$	B	65	0.085	0.99
$[Co(dpt)(dipic)]^{+/0}$	B	75	0.165	0.76[f]
$[Ru(NH_3)_5(pyraz\text{-}2,6\text{-}H_2)]^{3+/2+}$	C	55	0.585	0.98
$[Ru(NH_3)_5(pyraz\text{-}2,6)]^{+/0}$	D	105	0.455	0.74[f]
$[Fe(CN)_5(pyraz\text{-}2,6\text{-}H_2)]^{2-/3-}$	C	65	0.69	1.01
$[Fe(CN)_5(pyraz\text{-}2,6\text{-}H)]^{3-/4-}$	E	75	0.60	0.95
$[Fe(CN)_5(pyraz\text{-}2,6)]^{4-/5-}$	B	130	0.565	1.14[f]
$[(NH_3)_5Ru(\mu\text{-}pyraz\text{-}2,6)Co^{III}(dien)]^{4+/3+}$	C	68	0.72[d]	not determined[g]

[a] Vs. NHE. [b] At a scan rate of 50 mV s^{-1}. [c] Legend: A = 0.1 M KCl; B = 0.1 M $LiClO_4$; C = 0.1 M $HClO_4$; D = acetate buffer (0.2 M, pH 5.5); E = citrate buffer (pH 3.0). [d] Formal potential for the Ru(III)/Ru(II) couple. [e] Peak current ratio. [f] For derivations of peak current ratio from unity, see text. [g] See Figure 2a.

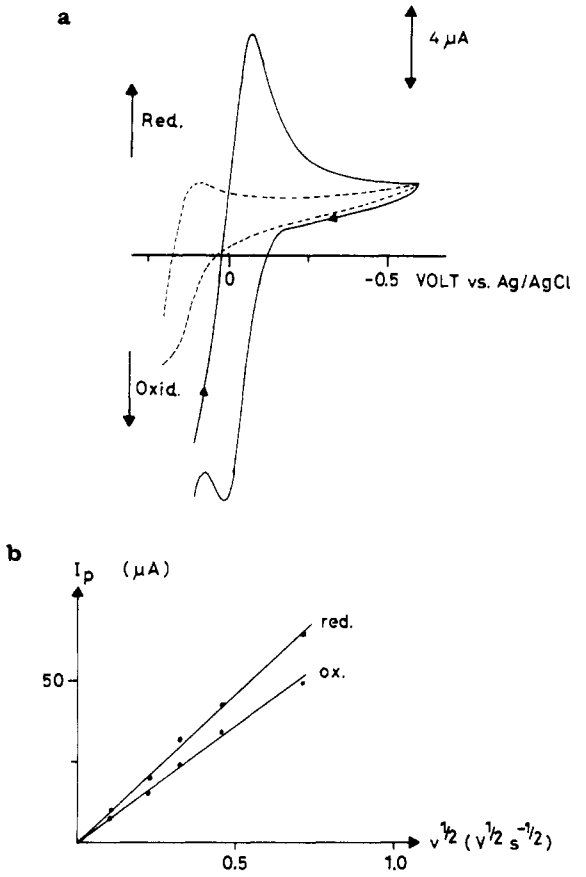

Figure 1. (a) Cyclic voltammogram of $[Co(dpt)(pyraz\text{-}2,6)]^{+/0}$ (0.1 M $LiClO_4$ electrolyte, hanging mercury drop electrode, scan rate 50 mV s^{-1}). The broken line is the cyclic voltammogram of the electrolyte measured under identical conditions. (b) Plot of cathodic and anodic peak currents vs. the square root of the scan rate.

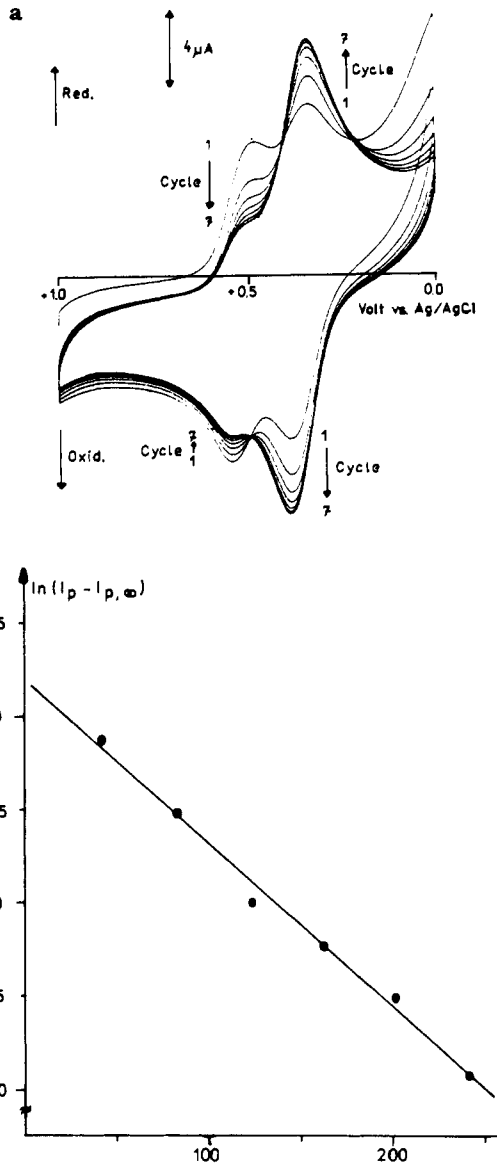

Figure 2. (a) Cyclic voltammogram of $[Ru(NH_3)_5(\mu\text{-pyraz-}2,6)\text{-}Co^{III}(dien)]^{4+}$ (0.1 M $HClO_4$, 3 °C, scan rate 50 mV s^{-1}, glassy-carbon electrode). (b) Plot of ln ($I_p - I_{p,\infty}$) vs. time for the reduction peak at a potential of 0.48 V vs. Ag/AgCl in the cyclic voltammogram given in (a).

mograms of cobalt complexes. The peak-current ratios $I_{p,a}/I_{p,c}$ are ~0.8 for all cobalt complexes. It has not been possible to determine these ratios very accurately due to the beginning oxidation of the mercury surface of the working electrode at potentials >0.3 V. Figure 1 shows a typical cyclic voltammogram and a plot of the anodic and cathodic peak currents vs. the square root of the scan rate for one of the more difficult cases (v = 10–500 mV s^{-1}). The couples $[Ru(NH_3)_5(pyraz\text{-}2,6\text{-}H_2)]^{3+/2+}$ and $[Fe(CN)_5(pyraz\text{-}2,6\text{-}H_2)]^{2-/3-}$ exhibit reversible cyclic voltammograms. The cyclic voltammograms of the fully deprotonated forms $[Ru(NH_3)_5(pyraz\text{-}2,6)]^{+/0}$ and $[Fe(CN)_5(pyraz\text{-}2,6)]^{4-/5-}$ are influenced by chemical equilibria in solution, which lead to a drastic increase of ΔE_p (105 and 130 mV, respectively). In both cases the redox potentials for the carboxylic groups in the fully protonated and deprotonated forms differ by approximately 0.127 V. The iron(III) complexes are always stronger oxidants than their Ru(III) counterparts as has been observed by Haim and Taube for similar couples.

The formal redox potential of Ru(III)/Ru(II) in the binuclear species $[(NH_3)_5Ru(\mu\text{-pyraz-}2,6)Co^{III}(dien)]^{4+}$ has been determined by cyclic voltammetry (Table II). Figure 2a shows a cyclic voltammogram of $[(NH_3)_5Ru^{III}(\mu\text{-pyraz-}2,6)Co^{III}\text{-}(dien)]^{4+}$ at 3 °C and at a relatively slow scan rate of 50 mV s^{-1}. Upon repeated scanning a new oxidation peak and a new reduction peak appear at more negative potentials, whereas the starting peaks disappear with time. The redox potential of +0.585 V derived from the new peaks is characteristic for the couple $[Ru(NH_3)_5(pyraz\text{-}2,6\text{-}H_2)]^{3+/2+}$, which is the monomeric product generated from the binuclear Ru(II)–Co(III) species after intramolecular reduction of the Co(III) center and rapid dissociation of the Co^{II}(dien) moiety. Thus, intramolecular electron transfer occurs on the time scale of the cyclic voltammetric measurements. A semilogarithmic plot of peak current vs. time at a peak potential of maximum change is linear (Figure 2b) for two half-lives at 3 °C, and a first-order rate constant of 0.008 s^{-1} may be deduced.[27] This agrees well with a value of 0.006 s^{-1} calculated from the activation parameters for the intramolecular electron transfer within $[(NH_3)_5Ru^{II}(\mu\text{-pyraz-}2,6)Co^{III}(dien)]^{3+}$.

Outer-Sphere Electron-Transfer Reactions of $[Co^{III}L_1L_2]^+$ Complexes. The endergonic reactions of $[Ru^{II}(NH_3)_5(pyraz\text{-}2,6\text{-}H_2)]^{2+}$ with various cobalt(III) complexes of the type $[Co^{III}L_1L_2]^+$ where L_1 = pyrazine-2,6-dicarboxylate, pyridine-2,6-dicarboxylate and L_2 = dien, dpt, 3 NH_3 afford the products $[Ru^{III}(NH_3)_5(pyraz\text{-}2,6\text{-}H_2)]^{3+}$, $[Co(H_2O)_6]^{2+}$, and uncoordinated protonated ligands L_1 and L_2 at $[H^+]$ = 0.1 M. Since both oxidant and reductant do not have labile coordination sites at either the Ru^{II} or Co^{III} center available, the mechanism of electron transfer is of the outer-sphere type. The

(27) It is assumed that diffusion of fresh binuclear precursor complex into the boundary layer at the electrode surface within the time of 10 scans (~1 min) is small and negligible.

Table III. Summary of Kinetic Parameters on the Outer-Sphere Oxidation of $[Ru^{II}(NH_3)_5(pyraz\text{-}2,6\text{-}H_2)]^{2+}$ by Various Complexes of Cobalt(III)

oxidant	k,[a] M^{-1} s^{-1}	$\Delta H^{\ddagger}$, kcal mol^{-1}	$\Delta S^{\ddagger}$, cal K^{-1} mol^{-1}	K_{12}
$[Co(NH_3)_3(pyraz\text{-}2,6)]^+$	4.16	8.0 ± 0.2	−28.7 ± 0.6	
$[Co(dien)(pyraz\text{-}2,6)]^+$ [b]	0.64	10.8 ± 0.4	−23 ± 1	8.95×10^{-5}
$[Co(dpt)(pyraz\text{-}2,6)]^+$	1.27	9.1 ± 0.1	−27.3 ± 0.3	1.8×10^{-6}
$[Co(dien)(dipic)]^+$	9.2×10^{-3}	17.1 ± 0.2	−10.4 ± 0.6	3.4×10^{-2}
$[Co(dpt)(dipic)]^+$	0.028	12.2 ± 0.4	−25 ± 1	1.6×10^{-3}

[a] Conditions unless otherwise stated: $I = 0.1$ M; $[H^+] = 0.1$ M $HClO_4$; 25 °C. [b] Conditions: $I = 0.1$ M; $[H^+] = 0.1$ M HCl.

Table IV. Exchange Rate Constants for $[CoL_1L_2]^+$ Complexes from the Marcus Equation at 25 °C, $I = 0.1$ M

reacn[c]	$k_{12,obsd}$,[a] M^{-1} s^{-1}	K_{12}[b]	f	$k_{2,calcd}$[d]	$k_{12,calcd}$, M^{-1} s^{-1}
$[Co(dien)(pyraz\text{-}2,6)]^+$	0.64	8.95×10^{-5}	0.6	3.4×10^{-3}	0.76
$[Co(dpt)(pyraz\text{-}2,6)]^+$	1.27	1.8×10^{-6}	0.3	0.74	1.13
$[Co(dien)(dipic)]^+$	9.2×10^{-3}	3.4×10^{-2}	0.9	0.7×10^{-9}	8.3×10^{-3}
$[Co(dpt)(dipic)]^+$	2.8×10^{-2}	1.6×10^{-3}	1.0	1.5×10^{-8}	8.8×10^{-3}

reacn	$k_{12,obsd}$, M^{-1} s^{-1}	K_{12}	f	$k_{12,calcd}$,[e] M^{-1} s^{-1}
$[Co(dien)(pyraz\text{-}2,6)]^0 + [Co(dpt)(pyraz\text{-}2,6)]^+$	0.30	40.7	0.94	0.31
$[Co(dien)(pyraz\text{-}2,6)]^+ + [Co(dpt)(pyraz\text{-}2,6)]^0$	8.7×10^{-3}	2.45×10^{-2}	0.85	7.2×10^{-3}

[a] Data from Table III. [b] Calculated from electrochemical data (Table II). [c] The reductant is $[Ru(NH_3)_5(pyraz\text{-}2,6\text{-}H_2)]^{2+}$. [d] In eq 6, 7, k_1 of $[Ru(NH_3)_5(pyraz\text{-}2,6\text{-}H_2)]^{2+}$ equals 3.2×10^6 M^{-1} s^{-1} at 25 °C, $I = 0.1$ M. [e] Calculated from eq 6, 7, by using the appropriate exchange rate constants from above.

Table V. Summary of Data on Intramolecular Electron Transfer in Binuclear Ru(II)–Co(III) and Fe(II)–Co(III) Complexes

precursor complex	k_{et},[a] s^{-1}	$\Delta H^{\ddagger}$, kcal mol^{-1}	$\Delta S^{\ddagger}$, cal K^{-1} mol^{-1}
$[(NH_3)_5Ru^{II}(pyraz\text{-}2,6)Co^{III}(dien)]^{3+}$ [b]	5.9×10^{-2}	18.4 ± 0.3	−2 ± 1
$[(CN)_5Fe^{II}(pyraz\text{-}2,6)Co^{III}(NH_3)_3]^{2-}$ [c]	4.1×10^{-2}	17.3 ± 0.3	−6 ± 1
$[(CN)_5Fe^{II}(pyraz\text{-}2,6)Co^{III}(dien)]^{2-}$ [d]	6.85×10^{-3}	30.0 ± 0.4	+32 ± 1.5
$[(CN)_5Fe^{II}(pyraz\text{-}2,6)Co^{III}(dpt)]^{2-}$ [e]	0.18	23.5 ± 0.5	+17 ± 1.5

[a] 25 °C. [b] Conditions: $I = 0.7$ M ($LiClO_4$); $[H^+] = 0.1$ M $HClO_4$; [ascorbate] = (0.5–5.0) × 10^{-3} M; at 600 nm. [c] Conditions: $I = 0.17$ M ($LiClO_4$); pH 5.5 (acetate buffer); [edta] = 5×10^{-4} M; [ascorbate] = 1×10^{-3} M; at 660 nm. [d] Conditons: $I = 0.12$ M ($LiClO_4$); pH 5.0 (acetate buffer); [edta] = 6×10^{-4} M; [ascorbate] = 2.3×10^{-3} M; at 620 nm. [e] Conditions: $I = 0.12$ ($LiClO_4$); pH 6.0 (acetate buffer); [edta] = 1×10^{-3} M; [ascorbate] = 2×10^{-4} M; at 640 nm.

kinetics of these reactions have been measured. A simple second-order rate law (eq 3) is found. The reactions are

$$-d[Ru^{II}]/dt = k[Co^{III}][Ru^{II}] \quad (3)$$

independent of acid concentration (0.01–0.1 M), which indicates the electron-transfer step to be rate determining rather than acid-catalyzed dissociation of $[Co^{II}L_1L_2]^0$ species.

Second-order rate constants and activation parameters are summarized in Table III. Detailed experimental kinetic data are available as supplementary material.

The inertness of $[Co^{II}L_1L_2]^0$ species in neutral aqueous solutions allows the experimental determination of the rate constants k_1 and k_{-1} of the equilibrium shown in eq 4, using

$$[(dien)Co^{II}(pyraz\text{-}2,6)]^0 + [(dpt)Co^{III}(pyraz\text{-}2,6)]^+ \underset{k_{-1}}{\overset{k_1}{\rightleftharpoons}} [(dien)Co^{III}(pyraz\text{-}2,6)]^+ + [(dpt)Co^{II}(pyraz\text{-}2,6)]^0 \quad (4)$$

pseudo-first-order conditions (excess $[(dpt)Co^{III}(pyraz\text{-}2,6)]^+$ for the elucidation of k_1; excess $[(dien)Co^{III}(pyraz\text{-}2,6)]^+$ for k_{-1}). Solutions of the Co(II) species were generated by reduction of the respective Co(III) complex with zinc amalgam at pH 7. At 25 °C and $I = 0.1$ M ($LiClO_4$), $k_1 = 0.3$ M^{-1} s^{-1}, $k_{-1} = 8.7 \times 10^{-3}$ M^{-1} s^{-1}, and $k_1/k_{-1} = K = 34.5$. The last value agrees well with a calculated value of $K = 40.7$, with use of the formal redox potentials (Table II) of both cobalt complexes.

Electron Transfer in $[(NH_3)_5Ru^{II}(\mu\text{-pyraz-2,6})Co^{III}(dien)]^{3+}$. The red binuclear $[(NH_3)_5Ru^{III}(\mu\text{-pyraz-2,6})Co^{III}(dien)]^{4+}$ cation is rapidly reduced to the corresponding blue Ru(II)–Co(III) species (Table I) by excess ascorbate in 0.1 M $HClO_4$.

This color fades slowly via intramolecular electron transfer as a new peak appears at 538 nm (log $\epsilon = 4.0$), which is characteristic of the final product $[Ru^{II}(NH_3)_5(pyraz\text{-}2,6\text{-}H_2)]^{2+}$. The latter complex has been recovered (95%) from such solutions after the reaction is completed by ion-exchange chromatography on a Sephadex column.

Scheme II

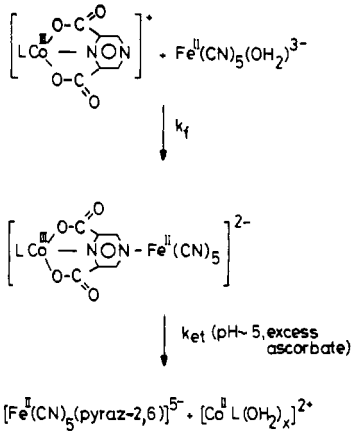

The intramolecular electron-transfer rate constants, k_{et}, measured at various temperatures are available as supplementary material. Activation parameters are listed in Table V.

Electron Transfer in $[(NC)_5Fe^{II}(\mu\text{-pyraz-2,6})Co^{III}L]^{2-}$ Species. Red cobalt(III) complexes of the type $[Co^{III}(pyraz\text{-}2,6)L]^+$ where L represents three NH_3 ligands, dien, and dpt react rapidly at pH 4.5–6 with $[Fe(CN)_5H_2O]^{3-}$ to afford deep blue solutions. The color is characteristic for metal to ligand charge-transfer bonds of complexes of pentacyanoferrate(II) with nitrogen heterocycles (Table I). A binuclear cobalt(III)–iron(II) precursor complex is formed (Scheme II), which undergoes intramolecular electron transfer with concomitant fading of the intense blue color.

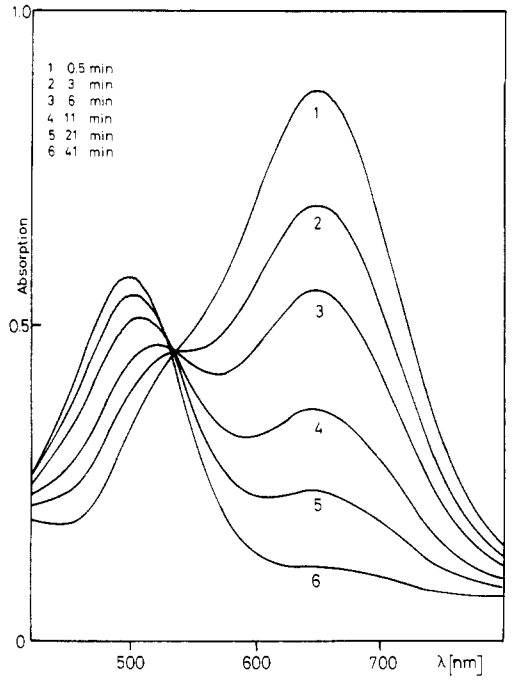

Figure 3. Scan spectra of the reaction of $[Fe^{II}(CN)_5OH_2]^{3-}$ (3×10^{-5} M) and $[Co^{III}(dien)(pyraz\text{-}2,6)]^+$ (2.5×10^{-4} M) at 15 °C (pH 4.8, acetate buffer; I = 0.12 M; [ascorbate] = 10^{-3} M).

The kinetics of the formation of the binuclear precursor complexes have not been studied in detail, but the formation is completed milliseconds after mixing of reactants.

Figure 3 shows a scan spectrum of the decay of $[(NC)_5Fe^{II}(\mu\text{-pyraz-}2,6)Co^{III}(dien)]^{2-}$ after its rapid formation from $[Fe^{II}(CN)_5OH_2]^{3-}$ (3.0×10^{-5} M) and excess $[Co(dien)(pyraz\text{-}2,6)]^+$ (2.5×10^{-4} M) at 15 °C and pH 4.8 (acetate buffer). The absorption maximum at 648 nm of the binuclear Fe(II)–Co(III) precursor fades whereas at 480 nm a new maximum appears, which is accounted for by the quantitative formation of $[Fe^{II}(CN)_5(pyraz\text{-}2,6)]^{5-}$ as reaction product. The complex anion has been quantitatively recovered from such solutions by cation-exchange chromatography on a Sephadex column.

An identical electronic spectrum has been obtained upon mixing of $[Fe^{II}(CN)_5H_2O]^{3-}$ (10^{-5} M) and pyrazine-2,6-dicarboxylic acid ($(1\text{–}10) \times 10^{-5}$ M). From these experiments it is concluded that under our experimental conditions the observed decay of the binuclear Fe(II)–Co(III) intermediate is achieved by intramolecular electron transfer (the primary $[Fe^{III}(CN)_5(pyraz\text{-}2,6)]^{4-}$ product is reduced by excess ascorbate); simple dissociation of the binuclear complex does not contribute significantly. The rate-determining step is therefore believed to be the intramolecular electron-transfer reaction.

Intramolecular rate constants and their respective activation parameters for the electron-transfer reaction within $[(NC)_5Fe^{II}(\mu\text{-pyraz-}2,6)Co^{III}L]^{2-}$ (L = 3 NH_3, dien, dpt) are summarized in Table V. Detailed kinetic data are available as supplementary material.

Outer-Sphere Oxidation of $[Fe^{II}(CN)_5(pyraz\text{-}2,6\text{-}H)]^{4-}$ by $[Co^{III}(dien)(pyraz\text{-}2,6)]^+$. The inertness of the $[Fe^{II}(CN)_5(pyraz\text{-}2,6)]^{5-}$ species in neutral aqueous solution makes the measurement of the kinetics of its oxidation by $[Co^{III}(dien)(pyraz\text{-}2,6)]^+$ feasible. Since oxidant and reductant do not have labile coordination sites available, this process is of the outer-sphere type. It was hoped that the relatively large negative charge of the reductant and the positive charge of the oxidant would lead to a large ion-pair formation constant, which would lead to a curvature in the plot of k_{obsd} vs. the concentration of the excess component $[Co(dien)(pyraz\text{-}2,6)]^+$

Scheme III

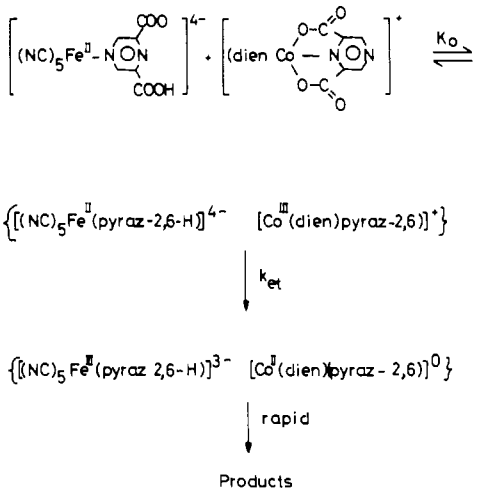

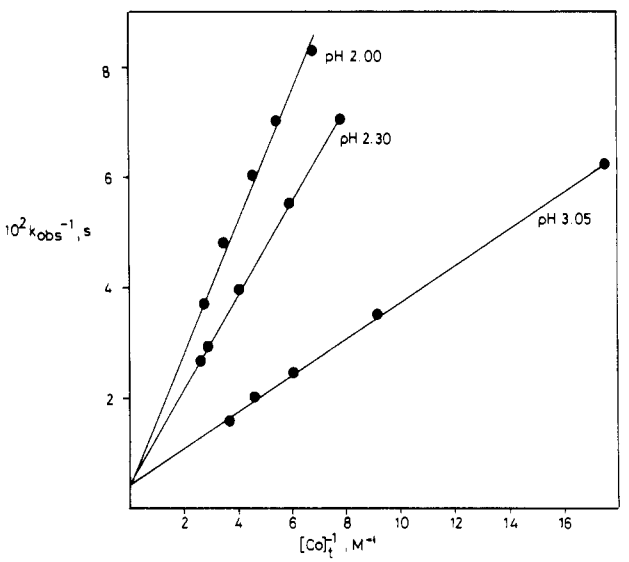

Figure 4. Plot of k_{obsd}^{-1} (s) vs. $[Co^{III}]^{-1}$ (M^{-1}) for the reaction of $[(NC)_5Fe^{II}(pyraz\text{-}2,6\text{-}H)]^{4-}$ with $[Co(dien)(pyraz\text{-}2,6)]^+$ at 25 °C.

and, thus, the intramolecular electron-transfer rate constant could be elucidated experimentally. A reaction sequence (Scheme III)—formation of a reactant ion pair (diffusion controlled), electron transfer (rate determining), and dissociation of the product pair (diffusion controlled)—leads to the rate law given by eq 5, if the oxidant is in excess and the

$$\frac{1}{k_{obsd}} = \frac{1}{k_{et}} + \frac{1}{k_{et}K_0[Ox]} \qquad (5)$$

reaction proceeds to completion. In order to ensure the last point, experiments were carried out in acidic solution (pH 2.0–3.0), since the endergonic reaction is driven to completion by rapid acid-catalyzed dissociation of the $[Co^{II}(dien)(pyraz\text{-}2,6)]^0$ product.

In the pH range between 2.0 and 3.0 the monoprotonated and diprotonated species are the dominant forms of the $[(CN)_5Fe(pyraz\text{-}2,6)]^{5-}$ complex. From the electrochemical measurements it is clearly shown that the monoprotonated species, $[(CN)_5Fe(pyraz\text{-}2,6\text{-}H)]^{4-}$, is the stronger reductant. A plot of k_{obsd}^{-1} vs. $[Ox]_t^{-1}$ (Figure 4) yields straight lines at a given $[H^+]$ with a common intercept (k_{et}^{-1}, s). At 25 °C $k_{et} = 3.9 \times 10^{-2}$ s^{-1} (I = 0.1 M). This is taken as experimental evidence that $[(CN)_5Fe(pyraz\text{-}2,6\text{-}H)]^{4-}$ reacts intramolecularly with the oxidant $[Co(dien)(pyraz\text{-}2,6)]^+$. The first protonation equilibrium can be observed spectrally by the bathochromic shifts of the visible-range bands. The spectral

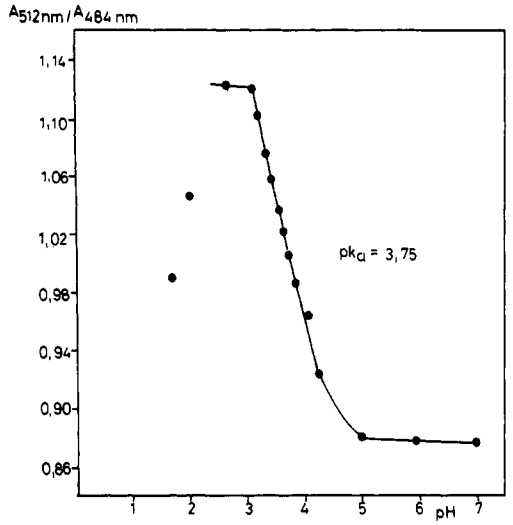

Figure 5. pK_a measurement for the protonation equilibrium of the $[(NC)_5Fe^{II}(pyraz\text{-}2,6)]^{5-}$ complex at 25 °C ($[Fe^{II}] = 4.3 \times 10^{-5}$ M).

difference between the unprotonated and monoprotonated species was used to determine the first protonation constant. A plot of solution pH vs. ratio of absorption at the wavelengths of the respective maxima gives a curve (Figure 5) from which a pK_a value of 3.8 was obtained. Thus, at pH 3.0 the monoprotonated species is the predominant species in solution. At high H^+ concentrations further protonations at cyanide ligands take place.[17]

Discussion

Self-Exchange Rates. The extensive body of thermodynamic and kinetic data on outer-sphere electron-transfer reactions between the various $[CoL_1L_2]^+$ oxidants and the common reductant $[Ru^{II}(NH_3)_5(pyraz\text{-}2,6\text{-}H_2)]^{2+}$ may be used to estimate electron-transfer self-exchange rate constants of the reactants. This has been done with use of the Marcus equation (eq 6, 7), where k_{12} is the rate constant for the cross-reaction, k_1 and k_2 are the exchange rate constants of the reactants, K_{12} is the equilibrium constant for the cross-reaction, and $Z = 10^{11}$ M^{-1}.

$$k_{12} = (k_1 k_2 K_{12} f)^{1/2} \quad (6)$$

$$\ln f = (\ln K_{12})^2/4 \ln (k_1 k_2/Z^2) \quad (7)$$

A reliable estimate of the exchange rate for $[Ru^{II}(NH_3)_5(pyraz\text{-}2,6\text{-}H_2)]^{2+}$ is obtained with use of the observed linear dependence of exchange rates for Ru–ammine complexes on the size of the reactants, which has been reported by Brown and Sutin.[28] They have shown that the inner-sphere reorganization energy (Franck–Condon factor ΔG_{in}) of ruthenium–ammine complexes is small and negligible as compared to the outer-sphere reorganization of solvent molecules (ΔG_{out}). Figure 6 shows the linear relation between the logarithm of observed exchange rates and the reciprocal of the mean distance of closest approach of the ruthenium centers. $\bar{a}$ for $[Ru(NH_3)_5(pyraz\text{-}2,6\text{-}H_2)]^{2+}$ was estimated by calculation of the radii equivalent to the sphere of equal volume, using the relation

$$\bar{a} = {}^1/_2(d_1 d_2 d_3)^{1/3} \quad (8)$$

where d_i values are the "diameters" along the three L–Ru–L axes. Values used for H_3N–Ru–NH_3, 6.6 Å, and H_3N–Ru–(pyraz-2,6-H_2), 15.8 Å, were estimated from molecular models and known crystallographic results. The calculated value of $1/\bar{r}$ for $[Ru(NH_3)_5(pyraz\text{-}2,6\text{-}H_2)]^{2+}$, where $\bar{r}$ is the mean distance of separation of the ruthenium centers, taken

(28) Brown, G. M.; Sutin, N. *J. Am. Chem. Soc.* **1979**, *101*, 883.

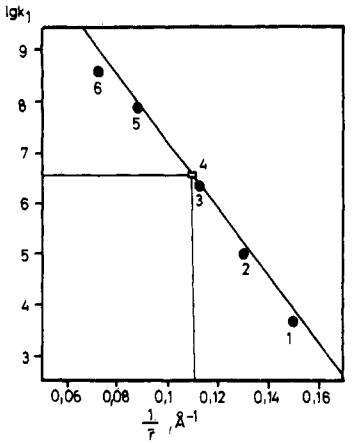

Figure 6. Plot of the logarithm of observed exchange rates vs. the reciprocal of the mean distance of closest approach of the ruthenium centers: (1) $[Ru(NH_3)_6]^{2+/3+}$; (2) $[Ru(NH_3)_5(py)]^{3+/2+}$; (3) $[Ru(NH_3)_4(bpy)]^{3+/2+}$; (4) $[Ru(NH_3)_5(pyraz\text{-}2,6\text{-}H_2)]^{2+/3+}$; (5) $[Ru(NH_3)_2(bpy)_2]^{3+/2+}$; (6) $[Ru(bpy)_3]^{2+/3+}$. Values were taken from ref 28 and references therein.

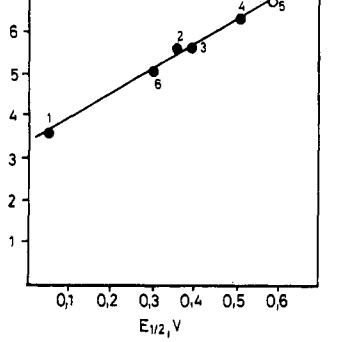

Figure 7. Correlation of electron-transfer self-exchange rates (k_1) at 25 °C of ruthenium–ammine complexes and their formal redox potentials ($E_{1/2}$): (1) $[Ru(NH_3)_6]^{2+/3+}$; (2) $[Ru(NH_3)_5(nic\text{-}H)]^{2+/3+}$; (3) $[Ru(NH_3)_5(isonic)]^{2+/3+}$; (4) $[Ru(NH_3)_4(bpy)]^{2+/3+}$; (5) $[Ru(NH_3)_5(pyraz\text{-}2,6\text{-}H_2)]^{2+/3+}$; (6) $[Ru(NH_3)_5(py)]^{2+/3+}$. Values for points 1, 2, 3, 4, and 6 were taken from ref 28 and references therein.

to be $2\bar{a}$, leads to an exchange rate constant for this complex of 3.2×10^6 M^{-1} s^{-1} at 25 °C and $I = 0.1$ M.

Another empirical linear correlation of exchange rates of ruthenium complexes vs. their respective redox potentials may be constructed with use of values from the literature (Figure 7). By use of the measured redox potential of 0.585 V for the couple $[Ru(NH_3)_5(pyraz\text{-}2,6\text{-}H_2)]^{3+/2+}$ an exchange rate constant of 3.2×10^6 M^{-1} s^{-1} is again extracted. It is now possible to calculate exchange rate constants of $[CoL_1L_2]^{+/0}$ complexes by using the Marcus equation (eq 6, 7) and the data in Table III. The best fit of measured values of the second-order rate constants of the cross-reactions, $k_{12,obsd}$, and calculated values, $k_{12,calcd}$, was obtained with use of the exchange rate constants for various $[CoL_1L_2]^{+/0}$ complexes in Table IV. Values for f were obtained by successive approximations.

Inspection of the exchange rates reveals that for complexes containing the ligand pyrazine-2,6-carboxylate the exchange rates are moderately fast whereas for complexes with the structurally quite similar ligand dipicolinate extremely slow exchange rates are observed. A reactivity difference of 6–7 orders of magnitude between $[Co(dien)(pyraz\text{-}2,6)]^{+/0}$ and $[Co(dien)(dipic)]^{+/0}$ or $[Co(dpt)(pyraz\text{-}2,6)]^{+/0}$ and $[Co(dpt)(dipic)]^{+/0}$ is apparent. It is not clear to us where this difference stems from since the Franck–Condon barriers of the two complexes should to a first approximation be rather

Table VI. Summary of Rate Data

complex	ref	$E_{1/2}$(Ru(III)/Ru(II)), V	k_{et}, s^{-1}	$\Delta H^{\ddagger}$, kcal mol^{-1}	$\Delta S^{\ddagger}$, cal mol^{-1} K^{-1}
$[(H_2O)Ru^{II}(NH_3)_4(isonic)Co^{III}(NH_3)_5]^{4+}$	4	0.39	0.012	19.7	−1.0
$[(SO_3)Ru^{II}(NH_3)_4(pyraz)Co^{III}(NH_3)_5]^{3+}$	5	0.64	0.128	22	+10.4
$[(SO_4)(NH_3)_4Ru^{II}(imz)Co^{III}(NH_3)_5]^{2+}$	5		6		
$[(NC)_5Fe^{II}(pyraz)Co^{III}(NH_3)_5]$	15		0.055	24.6	+18
$[(NC)_5Fe^{II}(pyraz)Co^{III}(NH_3)_4]^-$	15		0.013	22.7	+9.5
$[(NC)_5Fe^{II}(imz)Co^{III}(NH_3)_5]^-$	11		0.165	19.2	+2.4

similar (the O_2N_4-donor sets are very similar). However, the pyrazinedicarboxylate ligand is the better π-acceptor ligand as compared to dipicolinate, which may lower the inner-sphere reorganization energy. The kinetic and thermodynamic data of the outer-sphere reaction between $[Co^{III}(dpt)(pyraz\text{-}2,6)]^+$ and $[Co^{II}(dien)(pyraz\text{-}2,6)]^0$ have been measured (eq 4). If the Marcus equation (eq 6, 7) is applied to this system with use of the calculated exchange rates of Table IV for the two cobalt complexes and the measured equilibrium constant, K_{12}, excellent agreement between observed cross-reaction rate constants and calculated values is obtained (Table IV). This is good evidence that the Marcus equation adequately describes the kinetic and thermodynamic properties of these outer-sphere reactions and that our approach to estimate self-exchange rate constants leads to a consistent data set.

Intramolecular Electron-Transfer Reactions. The outer-sphere oxidation of $[Ru^{II}(NH_3)_5(pyraz\text{-}2,6\text{-}H_2)]^{2+}$ by $[Co^{III}L_1L_2]^+$ oxidants involves a rapid preequilibrium ion pairing or encounter complex formation characterized by an equilibrium constant, K_0, and a rate-determining electron-transfer step characterized by the first-order rate constant, k_{et}. Thus, the experimentally determined second-order rate constants (Table III) are composite values, $k = k_{et}K_0$. It is of interest to obtain an estimate of the intramolecular electron-transfer rate constant for the reaction of $[Ru^{II}(NH_3)_5(pyraz\text{-}2,6\text{-}H_2)]^{2+}$ with $[Co(dien)(pyraz\text{-}2,6)]^+$ because the analogous rate constant for the inner-sphere precursor $[(NH_3)_5Ru^{II}(\mu\text{-}pyraz\text{-}2,6)Co^{III}(dien)]^{3+}$ has been measured experimentally.

Using the well-known Eigen–Fuoss equation, it is possible to calculate K_0 according to eq 9. Definition of the parameters

$$K_0 = \frac{4\pi Na^3}{3000} \exp(-U(a)/k_BT) \qquad (9)$$

$$U(a) = Z_1Z_2e^2/Da(1 + \kappa a)$$

$$\kappa = (8\pi Ne^2I/1000Dk_BT)^{1/2}$$

are as follows: N, Avogadro's number; a, distance of closest approach; k_B, Boltzmann's constant; T, absolute temperature; Z_1 and Z_2, charges of ions 1 and 2, respectively; e, electronic charge; D, bulk dielectric constant of water, I, ionic strength.

With use of a distance of closest approach of 9.5 Å, a value of 1.6 M^{-1} for K_0 (25 °C, I = 0.1 M) for the above encounter complex formation constant has been calculated. This leads to an intramolecular electron-transfer rate constant of 0.4 s^{-1} at 25 °C within the ion pair $\{[Ru^{II}(NH_3)_5(pyraz\text{-}2,6\text{-}H_2)]^{2+}[Co^{III}(dien)(pyraz\text{-}2,6)]^+\}$.

This is significantly faster (by a factor of 7) than the analogous intramolecular electron transfer within the inner-sphere type precursor complex $[(NH_3)_5Ru^{II}(\mu\text{-}pyraz\text{-}2,6)\text{-}Co^{III}(dien)]^{3+}$. This difference in reactivity is satisfactorily accounted for by the differing driving forces of the two systems. From cyclic voltammetry measurements (Table II) it is clearly shown that the mononuclear ruthenium complex is the stronger reductant (by 135 mV) as compared to the Ru moiety in the binuclear Ru(II)–Co(III) analogue. If the relation $k_{et} \approx K_{eq}^{1/2}$ holds for the inner-sphere type reaction, this effect alone would predict a factor of 12 in favor of the reactivity of the outer-sphere encounter complex. This neglects the fact that most probably due to an enhanced electron delocalization within the binuclear Ru(II)–Co(III) complex the oxidizing capability of the Co^{III} center will be *reduced* to some extent as compared to that of its mononuclear analogue. Thus, the reactivity difference of a factor of 7 may be completely accounted for by differing driving forces of the two systems. This leads to the conclusion that the intramolecular electron transfers within the outer-sphere complex and the inner-sphere precursor are governed by the *same* energetic factors.

The inner-sphere type intramolecular electron transfer approaches or has already reached the adiabatic regime for pyrazine- or imidazolate-bridged Co^{III}–Ru^{II} complexes.[4,14] This has mainly been deduced from the fact that the entropies of activation are much the same within a series of bridged $Ru^{II}LCo^{III}(NH_3)_5$ complexes as are the enthalpies of activation. The present case fits this pattern (Table VI). This means that electron transfer within the outer-sphere encounter complex also approaches the adiabatic regime; i.e., there is also a sufficient amount of orbital coupling. It is conceivable that the necessary coupling may be achieved via some kind of stacking of the aromatic pyrazine rings of the oxidant and the reductant in the outer-sphere precursor complex:

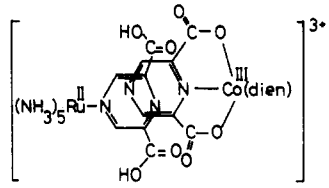

Similar behavior has been suggested for

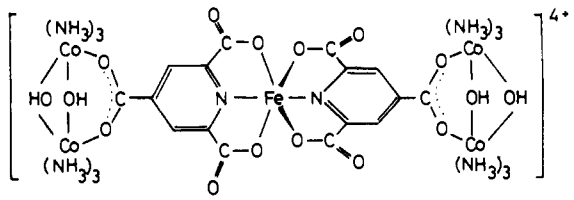

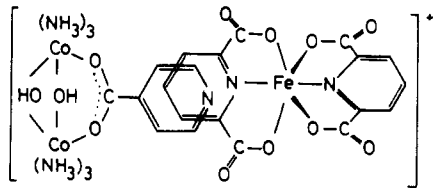

for which also very similar intramolecular electron-transfer rate constants have been measured.[29]

Intramolecular electron-transfer rate constants and the respective activation parameters are given in Table V for the systems

$$[(NC)_5Fe^{II}(\mu\text{-}pyraz\text{-}2,6)Co^{III}L]^{2-}$$

(L = 3 NH_3, dien, dpt). Some other pertinent data are summarized in Table VI.

(29) Bertram, H.; Wieghardt, K. *Inorg. Chem.* **1979**, *18*, 1799.

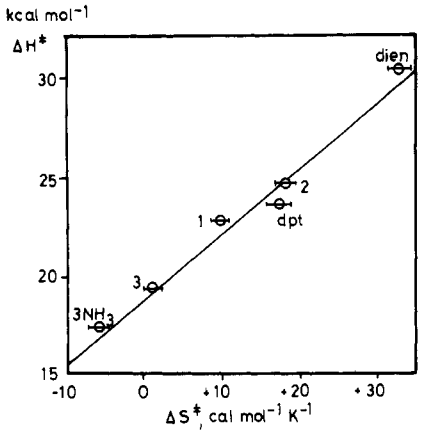

Figure 8. Isokinetic relationship for the intramolecular electron transfer in $[(NC)_5Fe^{II}(\mu\text{-pyraz-2,6})Co^{III}L]^{2-}$ (L = 3 NH_3, dien, dpt) and in (1) $[(NC)_5Fe^{II}(\text{pyraz-2})Co^{III}(NH_3)_4]^-$,[15] (2) $[(NC)_5Fe^{II}(\text{pyraz})Co^{III}(NH_3)_5]$,[15] and (3) $[(NC)_5Fe^{II}(\text{imz})Co^{III}(NH_3)_5]^-$.[11]

The above system allows us to systematically study the effect of nonmediating ligands coordinated at the oxidant on the intramolecular rate constant. The distances between the oxidizing Co(III) and the reducing Fe(II) centers are kept constant throughout the series since the bridging ligand is the same in all instances. Interestingly, the metal-to-ligand charge-transfer band of the $(NC)_5Fe^{II}$(pyraz-2,6) part is not affected by the different ligands L; the absorption maximum is observed around 650 (±10) nm for all three complexes, indicating that the nature of the reductant $(NC)_5Fe^{II}$(pyraz-2,6) remains unaffected.

From the data in Table V it is clear that a pronounced effect on the intramolecular rates is achieved by variation of L. When L is dpt, the fastest rate is observed (0.18 s^{-1}), followed by the system with L = 3 NH_3 (0.041 s^{-1}), and when L = dien, the slowest rate is observed (0.0068 s^{-1}) at 25 °C.

Rate comparisons at 25 °C are somewhat arbitrary because the activation parameters for the intramolecular electron-transfer processes in the three Fe^{II}–L–Co^{III} precursor complexes scatter considerably and no simple pattern is detectable (Tables V and VI). The Ru^{II}–L–Co^{III} systems in contrast exhibit a more rational pattern (small entropies of activation around zero and variation in the enthalpies of activation). This appears to be a feature of the systems with the $(NC)_5Fe^{II}$ moiety as reductant and has been reported previously.[14,15] Most disturbing is the large positive entropy of activation (+32 cal mol^{-1} K^{-1}) observed for $[(NC)_5Fe^{II}(\mu\text{-pyraz-2,6})Co^{III}(\text{dien})]^{2-}$, which may be compared with a value of +18 cal mol^{-1} K^{-1} observed for $[(NC)_5Fe^{II}(\mu\text{-pyraz})Co^{III}(NH_3)_5]^0$.[15] On the other hand, when the imidazolate bridge is operative, ΔS^* is reported to be +2.4 cal K^{-1} mol^{-1}.[11] Haim et al.[11,19] have attempted to rationalize the large positive entropies of activation on the basis of the charge redistribution concept (e.g., a solvent reorganization effect). It is also conceivable that these large variations are caused at least in part by experimental difficulties in determining activation parameters (the temperature range is generally quite small), but this is not considered to be the dominant source. A genuine effect is very likely to be operating. This is bolstered by the observation that an isokinetic relationship holds for data obtained by three independent groups (Figure 8). We are aware of the fact that the ΔG_0 range spanned by these systems is relatively small and the correlation should not be overinterpreted, but it may be indicative of a common reaction coordinate for all systems (limiting adiabatic intramolecular electron transfer).

As has been the case for the Co(III)–Ru(II) systems, a comparison is also possible for the Fe(II)–Co(III) systems between intramolecular electron-transfer rate constants of an inner-sphere precursor complex and its structurally very similar outer-sphere counterpart. But in contrast to the outer-sphere oxidation of $[Ru^{II}(NH_3)_5(\text{pyraz-2,6-H}_2)]^{2+}$ by $[Co(\text{dien})(\text{pyraz-2,6})]^+$ the *direct* determination of the intramolecular electron-transfer rate constant has been possible with use of the negatively charged $[Fe^{II}(CN)_5(\text{pyraz-2,6-H})]^{4-}$ reductant (k_{et} = 0.039 s^{-1} at 25 °C). Thus, the experimentally determined ratio k_{et}^{os}/k_{et}^{is} for the Co(III)–Fe(II) system is 5.6, which agrees satisfactorily with the value of 6.8 elucidated for the Ru(III)–Co(III) system. This suggests that the difference in reactivity may again be completely accounted for by the differing driving forces. The mononuclear Fe(II) species is most probably the stronger reductant, although direct measurement of the redox potential Fe(II)/Fe(III) in the binuclear species has in this instance not been possible. We conclude that the intramolecular electron transfer in both systems involving Fe(II)–Co(III) precursor complexes is in the adiabatic regime. A stacked structure of the ion pair $\{[(NC)_5Fe(\text{pyraz-2,6-H})]^{4-}/[Co(\text{dien})(\text{pyraz-2,6})]^+\}$ may allow a sufficient degree of coupling between oxidant and reductant.

Finally, it is noted that the rates of intramolecular electron transfer in $[(NH_3)_5Ru^{II}(\mu\text{-pyraz-2,6})Co^{III}(\text{dien})]^{3+}$ and in $[(NC)_5Fe^{II}(\mu\text{-pyraz-2,6})Co^{III}(\text{dien})]^{2-}$ differ by a factor of 9. The difference of the redox potentials for the couples $[Ru(NH_3)_5(\text{pyraz-2,6})]^{0/+}$ and $[(CN)_5Fe(\text{pyraz-2,6})]^{4-/5-}$ is 110 mV. Assuming the same difference for the binuclear species to be valid and k_{et} to vary with $K^{1/2}$, a factor, k_{et}^{Ru}/k_{et}^{Fe}, of 8.6 is calculated, which is in excellent agreement with the observed value. These interrelations of intramolecular electron-transfer rate and driving force differences have previously been used to argue that the actual electron transfer, k_1, in eq 10, is rate determining and not dissociation and/or spin change

$$M^{II}\text{–L–}Co^{III} \underset{k_{-1}}{\overset{k_1}{\rightleftharpoons}} M^{III}\text{–L–}Co^{II} \qquad (10)$$

$$Co^{II}\text{–L–}M^{III} \xrightarrow{k_2} \text{products} \qquad (11)$$

at the cobalt(II) center (eq 11). If eq 11 represents the rate-determining step ($k = K_1k_2$; $K_1 = k_1/k_{-1}$), the observed first-order rate constants would be expected to depend linearly on K_1[3,4,11,14] and a rate difference, k_{et}^{Ru}/k_{et}^{Fe}, of 73 would be predicted for eq 10 and 11.

Acknowledgment. Financial support of this research by the Deutsch Forschungsgemeinschaft and the Fonds der chemischen Industrie is gratefully acknowledged. A.N. is grateful for support by CAPES (Brazil).

Registry No. III, 91687-16-0; IVa, 91687-17-1; IVb, 91687-18-2; IVc, 91687-19-3; $[Co(NH_3)_3(\text{pyraz-2,6})]^+$, 91687-21-7; $[Co(\text{pyraz-2,6})(NH_3)_3](ClO_4)$, 91687-26-2; $[Co(\text{dien})(\text{pyraz-2,6})]^+$, 91687-22-8; $[Co(\text{pyraz-2,6})(\text{dien})](ClO_4)$, 91687-27-3; $[Co(\text{dpt})(\text{pyraz-2,6})]^+$, 91687-23-9; $[Co(\text{pyraz-2,6})(\text{dpt})](ClO_4)$, 91687-28-4; $[Co(\text{dien})(\text{dipic})]^+$, 47022-02-6; $[Co(\text{dipic})(\text{dien})]Cl$, 91741-07-0; $[Co(\text{dpt})(\text{dipic})]^+$, 91687-24-0; $[Co(\text{dipic})(\text{dpt})](ClO_4)$, 91687-29-5; $[Ru^{II}(NH_3)_5(\text{pyraz-2,6-H}_2)]^{2+}$, 91687-20-6; $[Ru(NH_3)_5(\text{pyraz-2,6-H}_2)](ClO_4)_2$, 91687-31-9; $[Ru^{II}(NH_3)_5(\text{pyraz-2,6})]^0$, 91687-30-8; $[Ru^{III}(NH_3)_5(\mu\text{-pyraz-2,6})Co(\text{dien})](ClO_4)_4$, 91687-33-1; $[Fe^{II}(CN)_5(\text{pyraz-2,6-H})]^{4-}$, 91687-25-1; $[Fe^{II}(CN)_5(\text{pyraz-2,6})]^{5-}$, 91687-34-2; $[Co(NH_3)_3(H_2O)Cl_2]Cl$, 13820-77-4; $[Co(\text{dien})Cl_3]$, 14215-59-9; $[Co(\text{dpt})Cl_3]$, 75918-15-9; $[Ru(NH_3)_5OH_2](PF_6)_2$, 34843-18-0; $[Fe^{II}(CN)_5OH_2]^{3-}$, 18497-51-3.

Supplementary Material Available: Listings of detailed kinetic data on the outer-sphere oxidation of $[Ru(NH_3)_5(\text{pyraz-2,6-H}_2)]^{2+}$ and $[(NC)_5Fe(\text{pyraz-2,6-H})]^{4-}$, intramolecular electron-transfer rate constants for $[(NH_3)_5Ru^{II}(\mu\text{-pyraz-2,6})Co^{III}(\text{dien})]^{3+}$ and $[(NC)_5Fe^{II}(\mu\text{-pyraz-2,6})Co^{III}L]^{2-}$ complexes, and elemental analyses (9 pages). Ordering information is given on any current masthead page.